Distribution of the ICI Term in Phase Noise Impaired OFDM Systems

Tim C. W. Schenk, *Member, IEEE*, Remco W. van der Hofstad, Erik R. Fledderus, and Peter F. M. Smulders, *Senior Member, IEEE*

***Abstract*— Orthogonality between the subcarriers of an orthogonal frequency division multiplexing (OFDM) system is affected by phase noise, which causes inter-carrier interference (ICI). The distribution of this interference term is studied in this paper. The distribution of the ICI for large number of carriers is derived and it is shown that the complex Gaussian approximation, generally applied in previous literature, is not valid and that the ICI term exhibits thicker tails. An analysis of the tail probabilities confirms these finding and shows that bit-error probabilities are severely underestimated when the Gaussian approximation for the ICI term is used, leading to too optimistic design criteria. Results from a simulation study confirm the analytical findings and show the validity of the limit distribution, obtained under the assumption of a large number of subcarriers, already for a modest number of subcarriers.**

***Index Terms*— Inter-carrier interference, limit distribution, orthogonal frequency division multiplexing, phase noise, stochastic integral, tail probabilities.**

I. Introduction

THE multicarrier technique orthogonal frequency division multiplexing (OFDM) [1] is chosen as basis for several wireless systems, because of its high spectral efficiency and ability to divide a dispersive multipath channel into parallel frequency flat subchannels. Furthermore, most systems apply a guard interval, a cyclic extension of the OFDM symbols, to protect the detected symbol against time delayed versions of the previous symbol, which could cause inter-symbol interference (ISI) [2]. OFDM is standardized for application in, amongst others, wireless local-area-networks (WLAN)[3], wireless metropolitan networks (WMAN), e.g. WiMAX [4], digital audio broadcasting (DAB) [5] and digital video broadcasting (DVB) [6].

Manuscript received August 4, 2005; revised March 14, 2006; accepted July 21, 2006. The associate editor coordinating the review of this paper and approving it for publication was M. Uysal. The work of T. C. W. Schenk, E. R. Fledderus, and P. F. M. Smulders was sponsored by the Dutch cooperative research project B4 BroadBand Radio@Hand (BTS01063). The work of R. W. van de Hofstad was supported in part by the Netherlands Organisation for Scientific Research (NWO).

T. Schenk was with the Telecommunications Technology and Electromagnetics Group, Eindhoven University of Technology, Eindhoven, P. O. Box 513, 5600 MB Eindhoven, The Netherlands. He is now with Philips Research Laboratories, Connectivity Systems and Networks Group, 5656 AE, Eindhoven, The Netherlands (e-mail: tim.schenk@philips.com).

R. van der Hofstad is with the Department of Mathematics and Computer Science, Eindhoven University of Technology, P. O. Box 513, 5600 MB Eindhoven, The Netherlands (e-mail: r.w.v.d.hofstad@tue.nl).

E. Fledderus, and P. Smulders are with the Telecommunications Technology and Electromagnetics Group, Eindhoven University of Technology, Eindhoven, P. O. Box 513, 5600 MB Eindhoven, The Netherlands (e-mail: e.r.fledderus@tue.nl; p.f.m.smulders@tue.nl).

Digital Object Identifier 10.1109/TWC.2007.05601.

The high spectral efficiency of OFDM is achieved by applying partly overlapping spectra for the different subcarriers. When the system is perfectly synchronized, these subcarriers are orthogonal. However, when due to imperfect local oscillators (LO) at either transmitter (TX) or receiver (RX) side of the system carrier frequency offset or phase noise (PN) occurs, the orthogonality between the subcarriers is lost and inter-carrier interference (ICI) occurs. These imperfections in the LOs will more and more appear to be a factor limiting performance of OFDM systems, when low-cost implementations or systems with high carrier frequencies are regarded, since it is in those cases harder to produce an oscillator with sufficient stability. Therefore, it is important to understand the influence of imperfect oscillators, i.e. phase noise, on the system performance.

The influence of PN on the performance of an OFDM system has been regarded in several publications, see e.g. [7]–[15]. They all show that the influence can be split into a multiplicative part, which is common to all subcarriers and therefore often referred to as common phase error (CPE), and an additive part, which is often referred to as inter-carrier interference (ICI). Although the CPE is identified as the main performance limiting factor for coherent detection based receivers, many adequate correction approaches for the CPE have been proposed previously, see, e.g. [8], [16], [17]. Some approaches for correction of the ICI have been proposed in [18], [19], which, however, require high signal-to-noise ratios (SNRs) to achieve reasonable performance and have a high complexity.

Thus, since any practical coherent OFDM receiver would have some kind of CPE correction, the main performance limiting factor in PN impaired systems is the ICI term. The properties of the ICI term are studied by several authors, see e.g. [7]–[11]. Many of these papers, implicitly or explicitly, assume the ICI term is complex Gaussian distributed, due to the central-limit-theorem. This is, however, as also noted by the authors of [14], [15], an approximation which is only valid for some combinations of PN and subcarrier spacings. The authors of [14] show that the complex Gaussian approximation only holds for *fast* PN, i.e., PN which changes fast compared to the symbol time, and that error probabilities calculated under this Gaussian assumption are very inaccurate for other types of PN. The authors of [15] confirm these findings with simulation results from Monte Carlo simulations, which show that good agreement with the Gaussian distribution is only achieved when the ratio of the -3 dB bandwidth of the power-spectral-density of the LO spectrum and the subcarrier spacing

approaches 1. It is noted, however, that these values of PN correspond to such a severe system performance degradation, that for practical systems this ratio always will be chosen to be much smaller than 1.

In this contribution we extend previous work by analytically studying the distribution of the ICI term due to PN in OFDM systems. We will derive a limit distribution for the ICI term, which will be shown to exhibit thicker tails than the complex Gaussian distribution with the same variance. We show that previous approaches, based on the Gaussian assumptions, significantly underestimate the tail probabilities of the ICI term, and thus underestimate the bit-error probabilities (BEP) of a system experiencing PN.

The paper is organized as follows. Section II introduces the system model and shows the influence of PN. In Section III we examine the distribution and tails of the ICI term for large number of carriers. Subsequently, we study the approximate distribution for small PN values. Additionally, simulation results are reported in this section to confirm the analytical findings. Finally, conclusions are drawn in Section IV.

II. OFDM System Experiencing PN

In this section we first derive the baseband system model for a system experiencing PN. Subsequently, we show how the induced ICI influences the BEP of such a system.

A. System Model

A transmitted OFDM signal is formed by applying the inverse discrete Fourier transformation (IDFT) to the complex data symbols and by adding a cyclic prefix to it by placing a copy of the last N_{G} samples in front of the symbol. This can be written as follows [1], [2]:

$$u_{m,n} = \begin{cases} \sqrt{\frac{1}{N}} \sum_{k=0}^{N-1} s_{m,k} \exp\left(i\frac{2\pi(n-N_{\text{G}})k}{N}\right) & \text{for } N_{\text{G}} \le n \le N_{\text{tot}} - 1 \\ u_{m,N+n} & \text{for } 0 \le n \le N_{\text{G}} - 1, \end{cases} \quad (1)$$

where we introduce

m	OFDM symbol index
n	sample index within the OFDM symbol, {0,1,...,N_{tot}-1}
N	number of subcarriers
k	subcarrier index, {0,1,...,N}
$u_{m,n}$	transmitted complex data signal during the nth sample of the mth symbol
N_{G}	the guard interval length
i	the imaginary unit, $i^2 = -1$
N_{tot}	OFDM symbol length $N + N_{\text{G}}$

Moreover, the transmitted complex data symbol during the mth symbol on the kth carrier is given by $s_{m,k}$, which can be rewritten as $s_{m,k} = R_{m,k} + iI_{m,k}$. We define R and I to be real zero-mean variables, which depend on the modulation scheme used for transmission. For instance, for BPSK modulation $R \in \{-1, 1\}$ with equal probability and $I = 0$. For QPSK or 4-QAM modulation $R \in \{-\frac{1}{\sqrt{2}}, \frac{1}{\sqrt{2}}\}$ and $I \in \{-\frac{1}{\sqrt{2}}, \frac{1}{\sqrt{2}}\}$, again with equal probability of occurrence.

The signal u is then up converted to radio frequency (RF) f_{RF} using the TX LO. Ideally this LO exhibits a spectrum which is given by a spectral line at f_{RF} and can be expressed by $\exp(i2\pi f_{\text{RF}} t)$. However, any practical LO will exhibit a random phase process, i.e., phase noise, and it is thus modeled as $\exp(i(2\pi f_{\text{RF}} t + \theta_{\text{TX}}(t)))$, where $\theta_{\text{TX}}(t)$ denotes the transmitter PN process, which is a function of time t.

At the RX side, the signal is down converted to baseband, by multiplication with the receiver local oscillator process $\exp(-i(2\pi f_{\text{RF}} t + \theta_{\text{RX}}(t)))$, where $\theta_{\text{RX}}(t)$ denotes the receiver PN process. Since we regard a sampled baseband model here, we further regard $\theta_{\text{TX},n}$ and $\theta_{\text{RX},n}$, which are the sampled versions of the TX and RX phase noise, respectively.

When we define $n' = mN_{\text{tot}} + n$, the received baseband signal with additive white Gaussian noise (AWGN) is given by

$$\begin{aligned} r_{m,n} &= u_{m,n} \exp\left(i(2\pi f_{\text{RF}} n' T + \theta_{\text{TX},n'})\right) \\ &\quad \cdot \exp\left(-i(2\pi f_{\text{RF}} n' T + \theta_{\text{RX},n'})\right) + w_{m,n} \\ &= u_{m,n} \exp\left(i\theta_{n'}\right) + w_{m,n}, \end{aligned} \quad (2)$$

where the combined TX and RX phase noise term is given by $\theta_n = \theta_{\text{TX},n} - \theta_{\text{RX},n}$ and $w_{m,n}$ denotes the complex Gaussian, zero-mean additive receiver noise with a variance of σ_w^2. Here we assumed the system does not experience a multipath channel.

Subsequently, the cyclic prefix is removed from $r_{m,n}$ by disregarding the first N_{G} samples of each symbol and the frequency domain complex data symbols are then found by applying the discrete Fourier transform (DFT) to the remaining samples, and are given by

$$x_{m,k} = \sqrt{\frac{1}{N}} \sum_{n=N_{\text{G}}}^{N_{\text{tot}}-1} r_{m,n} \exp\left(-i\frac{2\pi(n-N_{\text{G}})k}{N}\right). \quad (3)$$

Using (1) and (2), equation (3) can be rewritten as

$$x_{m,k} = g_{m,0} s_{m,k} + \sum_{l=0, l\neq k}^{N-1} g_{m,k-l} s_{m,l} + n_{m,k}, \quad (4)$$

where the received signal is split into three parts: the first term represents the signal term multiplied with the common phase error (CPE), the second is the inter-carrier interference (ICI) term caused by PN and the last term, i.e., $n_{m,k}$, models the AWGN in the frequency domain. The factor $g_{m,k-l}$ models the influence of the PN and is given by

$$g_{m,k-l} = \frac{1}{N} \sum_{n=0}^{N-1} \exp(i\theta_{mN_{\text{tot}}+N_{\text{G}}+n}) e^{-i\frac{2\pi(k-l)n}{N}}. \quad (5)$$

Here we define the increments of the phase noise process to be independent, which is the commonly used model for free-running oscillators [20], [21], so that

$$\theta_{n+1} = \theta_n + \varepsilon_{n+1} = \sum_{j=1}^{n+1} \varepsilon_j, \quad (6)$$

where $\theta_0 = 0$, $\varepsilon_n \sim \mathcal{N}\left(0, \sigma_\varepsilon^2\right)$ and $\sigma_\varepsilon^2 = 4\pi\beta T$. Here β denotes the one-sided -3 dB bandwidth of the corresponding Lorentzian spectrum of the LO and T is the sample time.

Since β is generally small compared to the subcarrier spacing $1/(NT)$, it is useful to define $\beta_{\mathrm{n}} = \beta NT$, which is the normalized version of β. Subsequently, we can rewrite σ_ε^2 as

$$\sigma_\varepsilon^2 = \frac{4\pi\beta_{\mathrm{n}}}{N} = \frac{\sigma^2}{N}, \tag{7}$$

where $\sigma^2 = 4\pi\beta_{\mathrm{n}}$ is independent of N.

Before detection is performed to $x_{m,k}$, generally correction of the CPE $g_{m,0}$ is applied. Approaches proposed in [8], [10], [16], [17] could be applied to do this. Remaining nuisances in detection of the signal are the common AWGN and the ICI term. The influence of the AWGN on detection is well known, but the statistical properties of the ICI term remain an open issue in previous literature. Therefore, the remainder of this paper will focus on the properties of this term.

The ICI for the kth carrier in the mth symbol, here denoted as $\xi_{m,k}$, is given by

$$\begin{aligned}
\xi_{m,k} &= \sum_{l=0,l\neq k}^{N-1} g_{m,k-l}s_{m,l} \\
&= \frac{1}{N}\sum_{l=0,l\neq k}^{N-1} s_{m,l}\sum_{n=0}^{N-1}\exp\left(i\theta_{mN_{\mathrm{tot}}+N_{\mathrm{G}}+n}\right)e^{-i\frac{2\pi(k-l)n}{N}} \\
&= \frac{1}{N}\sum_{l=0,l\neq k}^{N-1} s_{m,l}\sum_{n=0}^{N-1} e^{i\left(\sum_{j=1}^{mN_{\mathrm{tot}}+N_{\mathrm{G}}+n}\varepsilon_j\right)}e^{-i\frac{2\pi(k-l)n}{N}} \\
&= \frac{\chi_m}{N}\sum_{l=0,l\neq k}^{N-1} s_{m,l}\sum_{n=0}^{N-1} e^{i\left(\sum_{j=mN_{\mathrm{tot}}+N_{\mathrm{G}}}^{mN_{\mathrm{tot}}+N_{\mathrm{G}}+n}\varepsilon_j\right)}e^{-i\frac{2\pi(k-l)n}{N}} \\
&= \frac{\chi_m}{N}\sum_{l=0,l\neq k}^{N-1} s_{m,l}\sum_{n=0}^{N-1} e^{i\left(\sum_{j=0}^{n}\varepsilon'_j\right)}e^{-i\frac{2\pi(k-l)n}{N}},
\end{aligned} \tag{8}$$

where $\chi_m = \exp\left(i\sum_{j=1}^{mN_{\mathrm{tot}}+N_{\mathrm{G}}-1}\varepsilon_j\right)$, where the elements of ε'_j are i.i.d. according to $\mathcal{N}\left(0,\sigma_\varepsilon^2\right)$ and where $\{\varepsilon'_j\}_{j=0}^{N-1} = \{\varepsilon_{mN_{\mathrm{tot}}+N_{\mathrm{G}}+j}\}_{j=0}^{N-1}$ is independent of $\{\varepsilon_j\}_{j=1}^{mN_{\mathrm{tot}}+N_{\mathrm{G}}-1}$.

In the remainder of this paper we will, without loss of generality, regard the subcarrier $k = 0$ in symbol $m = 0$. When we then omit the subcarrier and symbol indices for brevity, (8) reduces to

$$\xi_{0,0} = \xi = \frac{\chi_0}{N}\sum_{l=1}^{N-1} s_l\sum_{n=0}^{N-1}\exp\left(i\sum_{j=0}^{n}\varepsilon'_j\right)\exp\left(i\frac{2\pi nl}{N}\right). \tag{9}$$

The random variable $\chi_0 = \exp\left(i\sum_{j=1}^{N_{\mathrm{G}}-1}\varepsilon_j\right)$ is independent of all other terms appearing in (9), and has norm 1 and, thus, gives rise to a rotation in the complex plane of the random variable

$$\frac{1}{N}\sum_{l=1}^{N-1} s_l\sum_{n=0}^{N-1}\exp\left(i\sum_{j=0}^{n}\varepsilon'_j\right)\exp\left(i\frac{2\pi nl}{N}\right). \tag{10}$$

For convenience, we will, therefore, in the sequel take $\chi_0 = 1$ and study (10), where we keep in mind that for the ICI, a random and independent rotation should be performed in the end.

B. Bit-Error Probabilities

We recall that the received signal after the DFT-processing $x_{m,k}$ is given by (4). Before detection is applied to this signal, first the CPE $g_{0,m}$ is removed. When this is assumed to be done perfectly, the resulting signal is given by

$$x' = s + \xi + n = s + \nu, \tag{11}$$

which is input to the decision device. Here ν denotes the additive error term. Note that the symbol and carrier index are omitted in (11) for brevity.

As a measure of performance of the system the symbol-error probability (SEP) can be considered, which is the probability that the output of the decision device for x' is incorrect. The SEP can be found by evaluating the probability of erroneous detection conditioned on the transmitted symbol for each of the symbols in the regarded modulation. The SEP can then be expressed as

$$P_{\mathrm{s}} = \frac{1}{M}\sum_{m=1}^{M}\left(1 - \mathbb{P}\left(x' \in \mathcal{R}_m | s = \mathcal{S}_m\right)\right), \tag{12}$$

where $\mathcal{R}_m$ is the decision region corresponding to the symbol $\mathcal{S}_m$ out of the modulation alphabet $\mathcal{S}$ with M elements. In a similar way the bit-error probability (BEP) can be evaluated, which can be expressed as

$$P_{\mathrm{b}} = \frac{1}{M}\sum_{m=1}^{M}\left(1 - \frac{1}{B}\sum_{b=1}^{B}\mathbb{P}\left(x' \in \mathcal{R}_{m,b} | s = \mathcal{S}_m\right)\right), \tag{13}$$

where $\mathcal{R}_{m,b}$ is the decision region corresponding to the bth bit of symbol $\mathcal{S}_m$. Clearly, (12) and (13) largely depend on the distribution of the error term ν. When ν consists of a complex normal distributed error source, i.e., when $\nu = n$, the expressions for (12) and (13) are well studied for different kind of modulations, see e.g. [22], [23]. For a system experiencing ICI due to PN, however, this is not the case, which justifies the study of the distribution of the term ξ in (10), as presented in Section III.

To further illustrate the dependence of the BEP on the distribution of the error term ν, we further work out (13) as an example for the QPSK or 4-QAM modulation, for which $M = 4$ and $B = 2$. It is easily verified that the BEP is given by (14). Here ν_{I} and ν_{R} denote the imaginary and real part of the error term ν, respectively. When only ICI is experienced, ν_{I} and ν_{R} can be replaced by ξ_{I} and ξ_{R} in (14), respectively. Here ξ_{I} and ξ_{R} denote the imaginary and real part of the ICI term ξ, respectively. The final expression for the BEP in (14) clearly illustrates the dependence of the system performance on the *tail probabilities* of the error term, i.e., the tail probabilities of the ICI-term in a PN-impaired system. The foregoing justifies a careful study of the tail probabilities of ξ, since they fully determine the system performance, as illustrated by (14). This study is presented in Section III-C.

III. Properties of the ICI Term

With the aim of deriving a statistical characterisation of the error term in detection of the transmitted symbols in a PN-

$$P_{\mathrm{b}}^{\mathrm{QPSK}} = \frac{1}{4}\left(4-\frac{1}{2}\left\{\left[\mathbb{P}\left(\nu_{\mathrm{I}}>-\frac{1}{\sqrt{2}}\right)+\mathbb{P}\left(\nu_{\mathrm{R}}<\frac{1}{\sqrt{2}}\right)\right]+\left[\mathbb{P}\left(\nu_{\mathrm{I}}>-\frac{1}{\sqrt{2}}\right)+\mathbb{P}\left(\nu_{\mathrm{R}}>-\frac{1}{\sqrt{2}}\right)\right]\right.\right.$$
$$\left.\left.+\left[\mathbb{P}\left(\nu_{\mathrm{I}}<\frac{1}{\sqrt{2}}\right)+\mathbb{P}\left(\nu_{\mathrm{R}}>-\frac{1}{\sqrt{2}}\right)\right]+\left[\mathbb{P}\left(\nu_{\mathrm{I}}<\frac{1}{\sqrt{2}}\right)+\mathbb{P}\left(\nu_{\mathrm{R}}<\frac{1}{\sqrt{2}}\right)\right]\right\}\right)$$
$$= \frac{1}{4}\left(\mathbb{P}\left(\nu_{\mathrm{I}}<-\frac{1}{\sqrt{2}}\right)+\mathbb{P}\left(\nu_{\mathrm{I}}>\frac{1}{\sqrt{2}}\right)+\mathbb{P}\left(\nu_{\mathrm{R}}<-\frac{1}{\sqrt{2}}\right)+\mathbb{P}\left(\nu_{\mathrm{R}}>\frac{1}{\sqrt{2}}\right)\right), \quad (14)$$

impaired system, we will, in this section, study the ICI term

$$\xi = \frac{1}{N}\sum_{l=1}^{N-1} s_l \sum_{n=0}^{N-1} \exp\left(i\sum_{j=0}^{n}\varepsilon_j'\right)\exp\left(i\frac{2\pi ln}{N}\right). \quad (15)$$

In Section III-A, we will study the convergence of ξ when $N\to\infty$. In Section III-B, we will study the distribution of the limit of ξ when σ is small, i.e., when the interference is quite small, and in Section III-C, we will qualitatively study the tails of the distribution when σ is small. Finally, in Section III-D we will investigate the BEP performance of a system impaired by PN by means of simulations and show how the derived distribution of ξ can be used to accurately predict the BEP performance.

A. Convergence of the ICI Term for Large N

Before stating the main convergence result, we need some notation and a key observation. We let $\{B_t\}_{t\geq 0}$ be a standard Brownian motion. Then, we have that

$$\{\varepsilon_j'\}_{j=0}^{N-1} \stackrel{d}{=} \left\{\sigma\left(B_{\frac{j+1}{N}}-B_{\frac{j}{N}}\right)\right\}_{j=0}^{N-1}, \quad (16)$$

where $X\stackrel{d}{=}Y$ when the random variables X and Y have the same distribution. Therefore, we have that

$$\xi \stackrel{d}{=} \frac{1}{N}\sum_{l=1}^{N-1} s_l \sum_{n=0}^{N-1} e^{i\frac{2\pi ln}{N}} \exp\left(i\sum_{j=0}^{n}\sigma\left(B_{\frac{j+1}{N}}-B_{\frac{j}{N}}\right)\right). \quad (17)$$

In the sequel, we will use $\varepsilon_j' = \sigma\left(B_{\frac{j+1}{N}}-B_{\frac{j}{N}}\right)$, and will identify the limit of the right-hand side of (17), which, for convenience, we again write as ξ.

We also define

$$\zeta = \sum_{l\in\mathbb{Z}:l\neq 0}\frac{\sigma s_l}{2\pi l}\int_0^1 e^{i\sigma B_t}[1-e^{i2\pi lt}]dB_t, \quad (18)$$

which will turn out to be the limit of ξ when $N\to\infty$.

Some words of caution are necessary here. The integral on the right-hand side of (18) is a so-called *stochastic integral*, which can be defined properly. In fact, the construction of such integral uses limits of the form in (17), and these ideas can be used to prove rigorously that the right-hand side of (17) converges to (18), as we will perform in more detail in the Appendix. Before continuing with the analysis, we list some properties of stochastic integrals that we will rely on. Firstly, we will use the rules that, for functions $f,g\colon[0,1]\times\mathbb{R}\to\mathbb{R}$ such that $\int_0^1\mathbb{E}[|f(t,B_t)|^2]dt, \int_0^1\mathbb{E}[|g(t,B_t)|^2]dt<\infty$, we have that

$$\mathbb{E}\Big[\int_0^1 f(t,B_t)dB_t\Big]=0, \quad (19)$$

and

$$\mathbb{E}\Big[\int_0^1 f(t,B_t)dB_t\int_0^1 g(t,B_t)dB_t\Big] = \int_0^1\mathbb{E}\big[f(t,B_t)g(t,B_t)\big]dt. \quad (20)$$

Secondly, we will use for any function $f\colon[0,1]\to\mathbb{R}$, we have that

$$\int_0^1 f(t)dB_t \quad (21)$$

has a normal distribution with mean zero and variance $\int_0^1 f^2(t)dt$. References for these statements can be found in [24, Chapter 13] or [25].

We will prove the following main result:

Theorem 3.1: When $N\to\infty$, for any $\sigma>0$ fixed, ξ in the right-hand side of (17) converges in probability to ζ, defined in (18).

The significance of Theorem 3.1 lies in the fact that it proves that the ICI converges when the number of subcarriers grows large, and it identifies the limit explicitly. In the sequel of this paper, we make use of this explicit limit ζ in (18) to derive properties of the ICI. We will also present simulations that show that the distribution of ξ is already close to the distribution of ζ when N equals 64, thus showing that the limit result in Theorem 3.1 is also of practical use.

The proof of Theorem 3.1 is deferred to the Appendix.

Simulation Results: To illustrate the convergence for large number of subcarriers in Theorem 3.1, we have carried out Monte Carlo simulations. In these simulations an OFDM system experiencing PN was simulated, where the PN was modeled as in (6). From the results of these simulation the ICI-term ξ, as expressed by (15) in the analysis above, was evaluated. The evaluation was carried out for QPSK modulation and a system for which all carriers were containing data symbols. As in the analytical derivations, no multipath channel was simulated. For all results 10^5 independent experiments were performed.

First Fig. 1 depicts the empirical cumulative distribution function (ECDF), denoted by $\mathrm{F}(x)$ in the figure, of the normalized real part of the ICI variable, i.e., of $\Re\{\xi\}/\sqrt{N}$, as found from these simulations. The results are given for $\sigma_\varepsilon^2 = 10^{-3}$. For a sample frequency of $f_{\mathrm{s}} = 1/T$, this means that the corner frequency of the PN spectrum β is given by $8.1\cdot 10^{-2}$ times the subcarrier spacing f_{s}/N. For an IEEE 802.11a based system [3], where the subcarrier spacing f_{s}/N equals 312.5 kHz, this corresponds to a β of 25.3 kHz. Results are depicted in the figure for systems

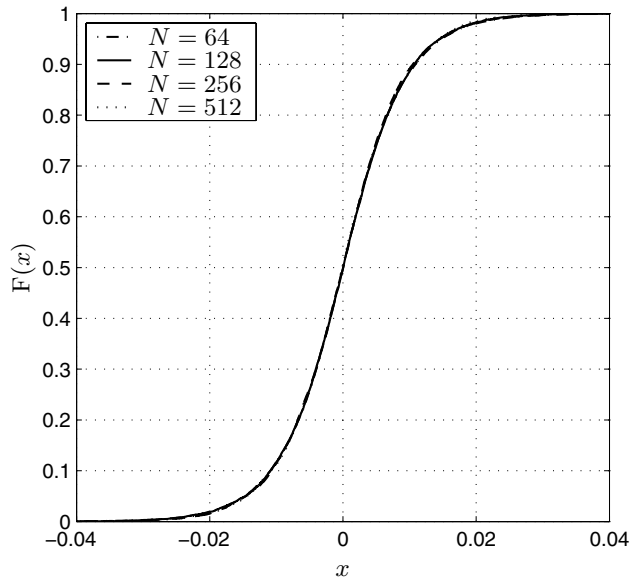

Fig. 1. The ECDF of the real part of the normalized ICI term, i.e., $\frac{\xi}{\sqrt{N}}$, found from Monte Carlo simulations of an OFDM system experiencing PN. The results are depicted for systems with different number of subcarriers N. The PN process was modeled according to (6) with a variance equal to $\sigma_\varepsilon^2 = 10^{-3}$.

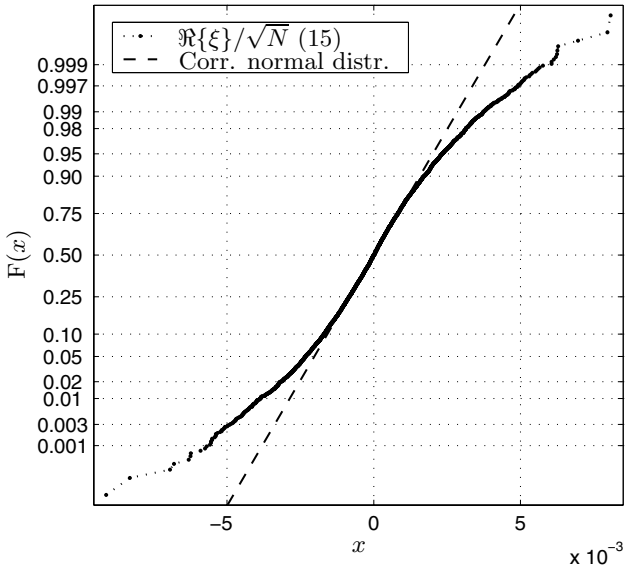

Fig. 2. Normal probability plot of the real part of the normalized ICI term, i.e., $\frac{\xi}{\sqrt{N}}$, found from Monte Carlo simulations of an OFDM system experiencing PN. The results are depicted for a system with $N = 512$ subcarriers. The PN process was modeled according to (6) with a variance equal to $\sigma_\varepsilon^2 = 10^{-3}$.

applying different number of carriers, i.e., for N equals 64, 128, 256 and 512.

From the results in Fig. 1 we can observe the convergence in distribution for high number of subcarriers N, as stated in the main result of Theorem 3.1 and proven in the Appendix. It is concluded that already for a moderate number of 64 subcarriers convergence seems to be reached, since all curves lie on top of each other. This shows that although the limit distribution was derived for high N, it is already applicable for moderate values of N. For the imaginary part of the ICI-term (15) the same convergence occurs.

The real part of the normalized ICI term is further studied in Fig. 2. Hereto the result of Fig. 1 for $N = 512$ subcarriers is depicted again, but now in a normal probability plot. This figure shows the distribution of the ICI with the corresponding normal distribution, i.e., the normal distribution with the same mean and variance. The scaling of the plot is such that a normal distribution would be depicted as a straight line.

It can be concluded from this graph that the ICI is clearly not normally distributed and that, since the curve is above and below the straight line in the left and right part of the figure, respectively, the ICI distribution has thicker tails than the normal distribution. Similar results were found for the imaginary part of the ICI. This result endorses the analytical results obtained in this section.

B. Approximation of the ICI for Small σ

In this section, we will investigate the distribution of the limit

$$\zeta = \sum_{l\in\mathbb{Z}:l\neq 0} \frac{\sigma s_l}{2\pi l} \int_0^1 e^{i\sigma B_t}[1 - e^{i2\pi lt}]dB_t. \tag{22}$$

Since the expression for the limit ζ is a stochastic integral it is difficult to apply it for analyses. Therefore we here regard the special case where σ is quite small. When this is the case, it seems reasonable to assume that we can replace $e^{i\sigma B_t}$ in (22) by 1. If we do so, then we end up with

$$\zeta \approx \sum_{l\in\mathbb{Z}:l\neq 0} \frac{\sigma s_l}{2\pi l} \int_0^1 [1 - e^{i2\pi lt}]dB_t = \sum_{l\in\mathbb{Z}:l\neq 0} \frac{\sigma s_l}{2\pi l}\Big[B_1 - \int_0^1 e^{i2\pi lt}dB_t\Big]. \tag{23}$$

We note that $Z = B_1$ is standard normally distributed, so that, with

$$X = \sum_{l\in\mathbb{Z}:l\neq 0} \frac{s_l}{2\pi l}, \tag{24}$$

we arrive at

$$\zeta \approx \sigma XZ - \sum_{l\in\mathbb{Z}:l\neq 0} \frac{\sigma s_l}{2\pi l} \int_0^1 e^{i2\pi lt}dB_t. \tag{25}$$

Next, since $t \mapsto e^{i2\pi lt}$ is deterministic, we have that $\int_0^1 e^{i2\pi lt}dB_t$ has a complex normal distribution. Furthermore, since, for $|k| \neq |l|$,

$$\mathbb{E}\left[\int_0^1 \cos(2\pi lt)dB_t \int_0^1 \cos(2\pi kt)dB_t\right] = \int_0^1 \cos(2\pi lt)\cos(2\pi kt)dt = 0, \tag{26}$$

we have that, with $Z_l = -\sqrt{2}\int_0^1 \cos(2\pi lt)dB_t$, the sequence $\{Z_l\}_{l=1}^\infty$ is a sequence of i.i.d. standard normal random variables, where we are using that a vector of normal random variables is independent when all covariances are equal to zero.

Similarly, we can see that, for $l \geq 1$, $Z_l' = -\sqrt{2}\int_0^1 \sin(2\pi lt)dB_t$ are i.i.d. standard normal

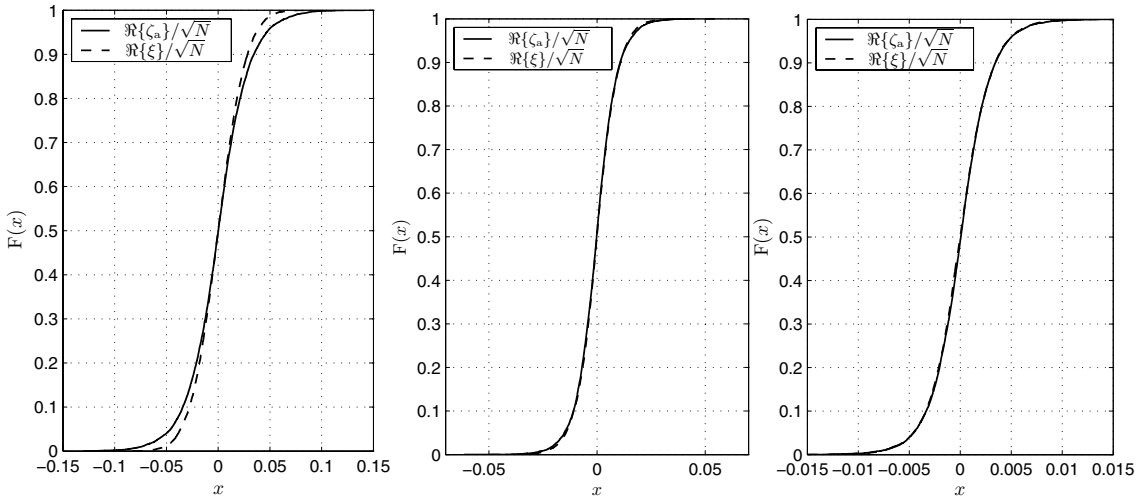

(a) $\sigma_\varepsilon^2 = 10^{-2}$ (b) $\sigma_\varepsilon^2 = 10^{-3}$ (c) $\sigma_\varepsilon^2 = 10^{-4}$

Fig. 3. The ECDF of the real part of the normalized ICI term, i.e., $\frac{\xi}{\sqrt{N}}$ (in dashed lines) and normalized real part of the approximation of the limit distribution for small σ_ε, i.e., $\frac{\zeta_a}{\sqrt{N}}$ (in solid lines). The results are depicted for $N = 512$ subcarriers and varying σ_ε^2.

variables. All these random variables are independent of $Z = B_1 = \int_0^1 dB_t$, since

$$\mathbb{E}\left[\int_0^1 \cos(2\pi lt) dB_t \int_0^1 1 dB_t\right] = \int_0^1 \cos(2\pi lt) dt = 0. \tag{27}$$

Finally, by a similar argument, also $\{Z_l\}_{l\geq 1}$ and $\{Z'_l\}_{l\geq 1}$ are independent. We conclude that

$$\zeta \approx \zeta_a = \sigma\big(ZX_1 + \frac{Y_{+,1} - Y_{-,2}}{2}\big) + i\sigma\big(ZX_2 + \frac{Y_{+,2} + Y_{-,1}}{2}\big), \tag{28}$$

where we define, with $s_l = R_l + iI_l$ for $l > 0$, and $s_l = R'_l + iI'_l$ for $l < 0$,

$$X_1 = \frac{1}{2\pi}\sum_{l=1}^{\infty}\frac{R_l + R'_l}{l}, \tag{29}$$

$$X_2 = \frac{1}{2\pi}\sum_{l=1}^{\infty}\frac{I_l + I'_l}{l}, \tag{30}$$

$$Y_{\pm,1} = \frac{1}{\sqrt{2}\pi}\sum_{l=1}^{\infty}\frac{Z_l[R_l \pm R'_l]}{l}, \tag{31}$$

$$Y_{\pm,2} = -\frac{1}{\sqrt{2}\pi}\sum_{l=1}^{\infty}\frac{Z'_l[I_l \pm I'_l]}{l}. \tag{32}$$

We note that for the bit-error probabilities (BEPs), we have to look at the probability that ζ is larger than a constant, say 1. This we can do when σ tends to zero, to investigate the BEPs when the interference decreases. We will investigate such probabilities in more detail in Section III-C.

Simulation Results: In the following we will numerically study ζ_a, as defined by (28), which is the approximation of the limit distribution of the ICI term ζ, as defined in (22), for small values of σ_ε.

Hereto Monte Carlo simulations were performed, in which, again, an OFDM system experiencing PN was simulated, where the PN was modeled as in (6). From the results of these simulations, the ICI-term ξ, as expressed by (15), was found. The evaluation was carried out for QPSK modulation and a system with $N = 512$ subcarriers that all contained data symbols. Furthermore, ζ_a was simulated using (28), also for QPSK modulation.

The results from these simulations for the normalized real part of the two resulting distributions are presented in Fig. 3, by means of their ECDF. The results are given in Fig. 3(a), Fig. 3(b) and Fig. 3(c) for σ_ε^2 equal to 10^{-2}, 10^{-3} and 10^{-4}, respectively. This corresponds to a -3 dB oscillator bandwidth β of $8.1 \cdot 10^{-1}$, $8.1 \cdot 10^{-2}$ and $8.1 \cdot 10^{-3}$ times the subcarrier spacing f_s/N, respectively. For all simulation results in this section, we have performed 10^5 independent experiments.

It can be concluded from Fig. 3 that the resemblance of the two distributions increases with decreasing β, which is as expected since ζ_a was derived under the assumption of small σ and, thus, small β. It is concluded that for the considered system already for $\sigma_\varepsilon^2 = 10^{-3}$ reasonable agreement between the CDFs seems to be achieved. This indicates that the approximate limit distribution ζ_a in (28) correctly models the distribution of the ICI for these values of σ_ε^2.

The ECDF of results from similar simulations, but now for $\sigma_\varepsilon^2 = 10^{-4}$, are given in Fig. 4. Here the ECDF is depicted on a logarithmic scale, which enables us to study the tails of the distributions. The figure, again, depicts the simulated real part of the normalized ICI of (15), the real part of the approximation of the limit distribution of the ICI term of (28), but now also the corresponding normal distribution, i.e., with the same mean and variance as the other variables. In Fig. 4, we have performed 10^6 experiments for each result.

It can be concluded from Fig. 4 that the limit distribution ζ_a well approximates the ICI, even in the tails of the distribution. Furthermore, it is found that the Gaussian distribution shows lower tail probabilities, and has a faster fall off. For instance, the probability that the real part of the normalized ICI is smaller or equal than -0.01 is approximately $2 \cdot 10^{-3}$, i.e., $\mathbb{P}(\xi \leq -0.01) \approx 2 \cdot 10^{-3}$. This is correctly predicted by

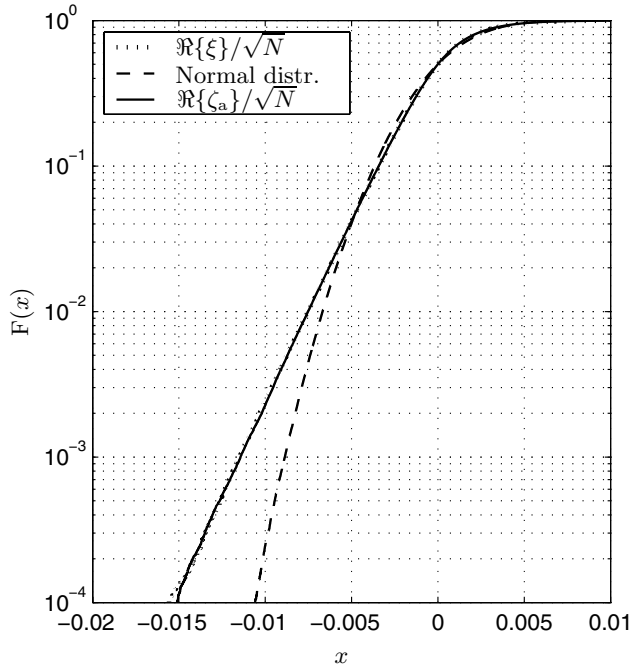

Fig. 4. The ECDF of the real part of normalized ICI term $\frac{\xi}{\sqrt{N}}$ (dotted line), as expressed in (15), and of the normalized approximation of the limit distribution $\frac{\zeta_a}{\sqrt{N}}$ (solid line), as expressed in (28), and of the corresponding normal distribution (dashed line) with the same mean and variance. Results are given for $N = 512$ subcarriers, QPSK modulation and a PN variance of $\sigma_\varepsilon^2 = 10^{-4}$.

the proposed limit distribution. The corresponding Gaussian approximation of the ICI, however, predicts the probability to be approximately $2 \cdot 10^{-4}$, which underestimates it by about a factor of 10.

C. Tail Probabilities

In this section, we will analytically show that the tail probabilities of the random variables in Section III-B are different from the ones for a Gaussian approximation, what was already numerically illustrated in Fig. 4. Tail probabilities are important in the ICI case since the BEP can be rewritten in terms of the tail probabilities, as was elucidated for QPSK in Section II-B. Therefore, a system with smaller tail probabilities performs better than a system with larger tail probabilities. We present a qualitative analysis of such tail probabilities in order to show that the usual Gaussian assumptions lead to an underestimation for the BEPs. This will be substantiated further by the results from appropriate BEP simulations in Section III-D.

We will start by computing the first two moments of the random variables appearing in (28):

$$\mathbb{E}[ZX_1] = \mathbb{E}[Y_{\pm,1}] = 0, \tag{33}$$

while, writing $\mathrm{Var}(R_1) = \sigma_{\mathrm{R}}^2$,

$$\begin{aligned}\mathbb{E}[(ZX_1)^2] &= \mathbb{E}[Z^2]\mathbb{E}[X_1^2] = \sigma^2\mathrm{Var}(X_1)\\ &= 2\sigma^2\mathrm{Var}(R_1)\sum_{l=1}^{\infty}\frac{1}{\pi^2 l^2} = 2\sigma^2\frac{\mathrm{Var}(R_1)}{6}\\ &= \frac{\sigma^2\sigma_{\mathrm{R}}^2}{3},\end{aligned} \tag{34}$$

and

$$\begin{aligned}\mathbb{E}[Y_{\pm,1}^2] &= \sigma^2\mathrm{Var}(R_1)\sum_{l=1}^{\infty}\frac{1}{\pi^2 l^2} = \frac{\sigma^2\mathrm{Var}(R_1)}{6}\\ &= \frac{\sigma^2\sigma_{\mathrm{R}}^2}{6}.\end{aligned} \tag{35}$$

Using further that $\mathbb{E}[ZX_1Y_{\pm,1}] = \mathbb{E}[ZX_1Y_{\pm,2}] = 0$, the random variable $\xi_{\mathrm{R}} = \sigma ZX_1 + \frac{\sigma}{2}(Y_{+,1} - Y_{-,2})$, which signifies the real part of the ICI, has mean zero and variance

$$\begin{aligned}\mathrm{Var}(\xi_{\mathrm{R}}) &= \sigma^2\mathbb{E}[(ZX_1)^2] + \frac{1}{4}\big(\mathbb{E}[Y_{+,1}^2] + \mathbb{E}[Y_{-,2}^2]\big)\\ &= \sigma^2\sigma_{\mathrm{R}}^2\left(\frac{1}{3} + \frac{1}{12}\right) = \frac{5\sigma^2\sigma_{\mathrm{R}}^2}{12}.\end{aligned} \tag{36}$$

Therefore, the usual Gaussian assumptions lead to a tail estimate of the form

$$\mathbb{P}(\xi_{\mathrm{R}} > y) \approx Q\left(\frac{y}{\sigma}\right) = \exp\left(-\frac{6y^2}{5\sigma^2\sigma_{\mathrm{R}}^2}(1 + o(1))\right). \tag{37}$$

We will now show that the tail is in fact much larger than that.

In the explanation below, we will assume that R_l and I_l are ± 1 with equal probability, for which $\sigma_{\mathrm{R}}^2 = 1$. For this, we fix a P, and we investigate the probability that $R_l = R_l' = 1$ for $l \le P$, while $\sum_{l>P}\frac{R_l + R_l'}{l} \ge 0$ and $Y_{+,1} + Y_{-,2} \ge 0$. By symmetry of the random variables involved, this probability is at least $\frac{1}{4^P} \cdot \frac{1}{2} \cdot \frac{1}{2}$. Also, when the above is true, then

$$X_1 \ge \sum_{l=1}^{M}\frac{1}{\pi l} = \frac{1}{\pi}\log P(1 + o(1)). \tag{38}$$

Therefore, in order for $\sigma ZX_1 \ge y$ to hold, we only need that

$$Z \ge \frac{\pi y}{\sigma \log P}, \tag{39}$$

which has probability

$$Q\left(\frac{\pi y}{\sigma\log P}\right) \sim \exp\left(-\frac{\pi^2 y^2}{2\sigma^2\log^2 P}(1 + o(1))\right). \tag{40}$$

Therefore, for every $P \ge 1$ and $y > 0$,

$$\mathbb{P}(\xi_{\mathrm{R}} > y) \ge \frac{1}{4^P}\cdot\frac{1}{4}\exp\left(-\frac{\pi^2 y^2}{2\sigma^2\log^2 P}(1 + o(1))\right). \tag{41}$$

For example, for $P = \frac{y^2}{\sigma^2\log^4(\frac{y}{\sigma})}$, we obtain that $\frac{1}{4^{P+1}} = \exp\big(o(\frac{y^2}{\sigma^2\log^2 P})\big)$, so that

$$\mathbb{P}(\xi_{\mathrm{R}} > y) \ge \exp\left(-\frac{\pi^2 y^2}{8\sigma^2\log^2(\frac{y}{\sigma})}(1 + o(1))\right). \tag{42}$$

The tail in (42) is much larger than the ones in (37), so that Gaussian assumptions, as formulated in (37), lead to a systematic underestimation of the tails, and therefore of the BEPs. Indeed, when $y = 1$ and σ is quite small, the exponent has become a factor $\frac{48\log^2(\frac{1}{\sigma})}{5\pi^2}$ smaller, which is substantial for σ small. This can be clearly seen in the results from simulations in Fig. 2, where we see thicker tails of the ICI distribution compared to a normal random variable with the same variance. This is even more clear from the ECDF depicted on a logarithmic scale in Fig. 4. A similar analysis could be carried out for the imaginary part of the ICI ξ_{I}.

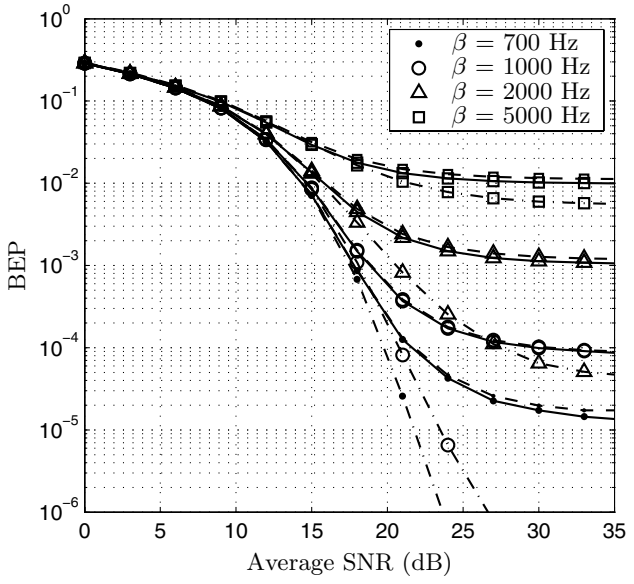

Fig. 5. BEP results from Monte Carlo simulations with an IEEE 802.11a-like system applying 16-QAM modulation. Results are included for: a system experiencing PN modeled as in (6) for different values of β and applying perfect CPE correction (in dashed lines), a system modeling the resulting ICI as an equivalent complex Gaussian process (in dash-dot lines) and a system modeling the resulting ICI according to the small σ approximation of the limit distribution as in (28) (in solid lines).

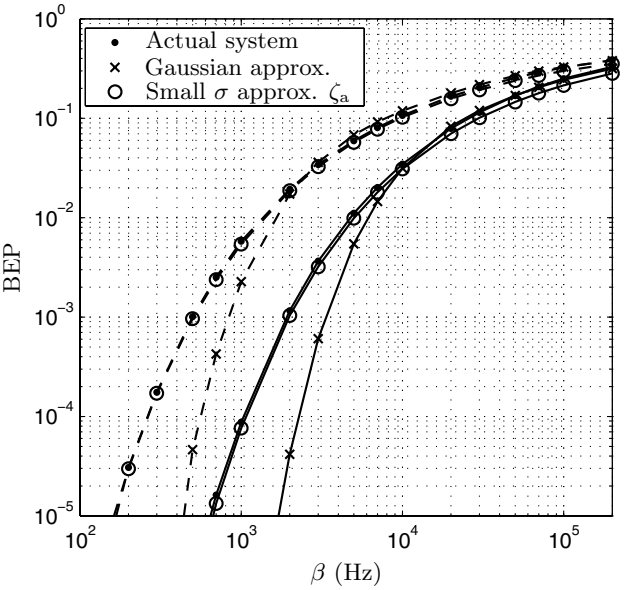

Fig. 6. BEP results from Monte Carlo simulations with an IEEE 802.11a-like system applying 16-QAM (in solid lines) and 64-QAM (in dashed lines) modulation. Results are included for: a system experiencing PN modeled as in (6) for different values of β and applying perfect CPE correction (*Actual system*), a system modeling the resulting ICI as an equivalent complex Gaussian process (*Gaussian approx.*) and a system modeling the resulting ICI according to the small σ approximation of the limit distribution as in (28) (*Small σ approx. ζ_a*).

D. Simulation Results

To confirm these analytical findings, we have carried out BEP simulations. Hereto an IEEE 802.11a-like system was simulated, i.e., the number of carriers N = 64, guard interval length N_G = 16 samples, the sample frequency f_s = 20 MHz, which corresponds to a sample length of 50 ns and a symbol length of (64+16)·50 ns = 4 μs. In the system all 64 subcarriers contain data symbols, which for Fig. 5 are taken from the 16-QAM modulation alphabet and for Fig. 6 from both the 16-QAM and 64-QAM modulation alphabet. A system without coding and not experiencing a multipath channel was simulated. The packet length in the simulations was equal to 10 symbols.

Fig. 5 shows BEP results for a system impaired by both AWGN and PN. The BEP is depicted versus the signal-to-noise ratio (SNR) for different values of β, i.e., the -3 dB bandwidth of the LO power spectral density. The PN is generated according to the model in (6) and the CPE is perfectly removed, leaving the ICI as the only influence of the PN. Results from these simulations are given by the dashed lines in the figure. The simulated βs vary from 700 to 5000 Hz, which corresponds to σ_ε^2 values varying from $1.4\pi \cdot 10^{-4}$ to $\pi \cdot 10^{-3}$.

These results are depicted together with results from simulations where the influence of the ICI is modeled as an additional zero-mean complex Gaussian noise source at the receiver, i.e., the commonly used approach in previous literature, where the variance of the noise equals that of the actual ICI. The results of these simulations are given by the dash-dot lines. Finally, results are included from simulations where the influence of the ICI is modeled using the small σ approximation of the proposed model for ICI, i.e., ζ_a, as defined by (28). These results are depicted by solid lines.

It can be concluded from Fig. 5 that the BEP is severely underestimated using the Gaussian approximation for the ICI term. Especially for small values of β, i.e., small σ values, the difference between the actual and predicted BEP by the Gaussian model are very large, which confirms our analytical findings on tail probabilities in the previous section. For instance for β = 2000 Hz and a SNR of 30 dB the BEP is underestimated by a factor of 20 using the Gaussian approach. For lower values of β this difference is even higher. The resulting BEPs using the approximate of the proposed limit distribution, in contrast, closely resemble those of the actual PN impaired system. It is noted that this limit distribution was found under the assumption of a large number of carries, but, judging the results, it already holds for a system with a modest number of 64 subcarriers.

Results depicted in Fig. 6 are obtained from similar simulations carried out for a system not experiencing additive RX noise, i.e., the system is only impaired by PN. Results from BEP simulations, for the same three cases as for Fig. 5, are depicted versus β for both the 16-QAM (in solid lines) and 64-QAM (in dashed lines) modulation. These results can be interpreted as the high SNR flooring of the BEP curve for a certain β, i.e., the maximum achievable BEP performance for a certain level of PN.

It can be concluded from Fig. 6 that for both modulation formats the Gaussian approximation of the ICI only provides reliable BEP results for very high values of β, where the BEP is so high that reliable data transfer is almost not possible. This confirms findings previously presented in [14] and [15], where simulations were used to show the validity of the Gaussian model for the ICI only for very large values of β. The BEPs

found from simulations with ζ_a, the approximate expression for our limit distribution ζ, on the other hand, show good agreement with the BEPs found from simulations with the actual PN impaired system. It is noted though that a small discrepancy occurs at high values of β, where σ becomes high, since the approximate results of Section III-B were derived for small σ. The results are, however, even for these high β values reasonable. For these high values of β the actual evaluation of ζ in (18) will obtain better results.

Overall it can be concluded from the simulation results in this section that, although derived for large N and small σ, the approximate limit distribution ζ_a can be well applied to find the BEP of a PN-impaired system. It is noted, furthermore, that simulations were carried out for a system with a low number of carriers, i.e., $N = 64$, and that the applicability of our results will even be better for systems with higher number of subcarriers like, e.g., WiMAX, DVB and DAB, since for these kind of systems N is much larger and the typically permissible σ is considerably lower.

IV. Conclusions

The wide application of orthogonal frequency division multiplexing (OFDM) in wireless systems justifies a careful investigation of its performance limiting factors. The influence of imperfect oscillators, i.e., phase noise (PN), is identified as one of the major impairments of OFDM, especially when low-cost and high-frequency systems are considered. Therefore, the distribution of the inter-carrier interference (ICI) due to PN is studied in this paper.

In most of the previous contributions, the ICI was assumed to be zero-mean complex Gaussian distributed. In this paper, however, it was shown that this assumption is not valid and the limit distribution of the ICI term for large number of subcarriers is derived. This distribution is shown to exhibit thicker tails than the Gaussian distribution with the same mean and variance. In an analysis of the tail probabilities these finding were confirmed and it was shown that bit-error probabilities are severely underestimated when the Gaussian approximation for the ICI term is used.

Results from simulation studies show the validity of the limit distribution, obtained under the assumption of a large number of subcarries, already for a modest number of subcarriers. Furthermore, they show that for small values of the PN variance, the limit distribution very well resembles the ICI distribution. Additionally, it is shown that the tail probabilities are severely underestimated by the corresponding Gaussian distribution. Finally, results from a BEP-study for a IEEE 802.11a-like system show that the derived limit distribution is suitable to obtain the correct BEP of a PN-impaired system, this in contrast to an approach using the Gaussian approximation.

The results in this paper can be used by system designers to better specify the level of tolerable PN, for an OFDM system to achieve a certain bit-error probability. This paper shows that applying the Gaussian approximation would lead to a serious underspecification of the LO.

Appendix

In this Appendix we will provide the proof for Theorem 3.1. We first reduce the proof of Theorem 3.1 to four key convergence statements (52), (59), (65) and (66). After this, we prove these four statements separately.

Proof of Theorem 3.1 subject to (52), (59), (65) and (66). We recall that X_N converges in probability to X, and write $X_N \xrightarrow{P} X$, when, for every $\epsilon > 0$,

$$\lim_{N\to\infty} \mathbb{P}(|X_N - X| > \epsilon) = 0. \tag{43}$$

We will make frequent use of the fact that if X_N and Y_N converge in probability to X and Y, then also $X_N + Y_N$ converges to $X + Y$ in probability.

We start by rewriting the sum

$$\sum_{n=0}^{N-1} e^{i\sum_{j=0}^{n}\varepsilon'_j} e^{i\frac{2\pi ln}{N}}. \tag{44}$$

For this, we will use *partial summation*, which states that for any two sequences of numbers $\{a_n\}_{n=1}^{m}$ and $\{b_n\}_{n=1}^{m}$, we have

$$\sum_{n=0}^{m-1} a_n(b_{n+1} - b_n) = a_m b_m - a_0 b_0 - \sum_{n=0}^{m-1}(a_{n+1} - a_n)b_{n+1}. \tag{45}$$

We apply this to

$$a_n = e^{i\sum_{j=0}^{n}\varepsilon'_j}, \qquad b_{n+1} - b_n = e^{i\frac{2\pi ln}{N}}, \tag{46}$$

so that

$$b_n = \sum_{j=0}^{n-1} e^{i\frac{2\pi lj}{N}}. \tag{47}$$

For this choice, we can compute that $b_0 = b_N = 0$, and

$$b_n = \frac{e^{i\frac{2\pi ln}{N}} - 1}{e^{i\frac{2\pi l}{N}} - 1}. \tag{48}$$

Therefore, we arrive at

$$\sum_{n=0}^{N-1} e^{i\sum_{j=0}^{n}\varepsilon'_j} e^{i\frac{2\pi ln}{N}} = \frac{1}{e^{i\frac{2\pi l}{N}} - 1} \sum_{n=0}^{N-1} \left[e^{i\varepsilon'_{n+1}} - 1\right] e^{i\sum_{j=0}^{n}\varepsilon'_j} \left[1 - e^{i\frac{2\pi l(n+1)}{N}}\right]. \tag{49}$$

Now, ε'_{n+1} is small, since it has variance $\sigma_\varepsilon^2 = \frac{\sigma^2}{N}$. Therefore, we can expand $e^{i\varepsilon'_{n+1}} - 1 \approx i\varepsilon'_{n+1}$ to arrive at

$$\sum_{n=0}^{N-1} e^{i\sum_{j=0}^{n}\varepsilon'_j} e^{i\frac{2\pi ln}{N}} \approx \frac{i}{e^{i\frac{2\pi l}{N}} - 1} \sum_{n=0}^{N-1} \varepsilon'_{n+1} e^{i\sum_{j=0}^{n}\varepsilon'_j} \left[1 - e^{i\frac{2\pi l(n+1)}{N}}\right]. \tag{50}$$

Using (50) we define an approximation of ξ given by

$$\xi' = \sum_{l=1}^{N-1} \frac{is_l}{N[e^{i\frac{2\pi l}{N}}-1]} \sum_{n=0}^{N-1} \varepsilon'_{n+1} e^{i\sum_{j=0}^{n}\varepsilon'_j} \big[1 - e^{i\frac{2\pi l(n+1)}{N}}\big]. \tag{51}$$

Indeed, below we will prove that, η_N, which is defined to be the difference between ξ and ξ', converges to zero in probability, i.e.,

$$\eta_N = \xi - \xi' \xrightarrow{P} 0, \tag{52}$$

in probability. Therefore, to prove the claim, it now suffices to prove that $\xi' \xrightarrow{P} \zeta$.

When we use the periodicity of $e^{i\frac{2\pi ln}{N}}$ and $e^{i\frac{2\pi l}{N}}$, we can more conveniently rewrite ξ' as

$$\xi' \approx \sum_{0<|l|\le N/2} \frac{is_l}{N[e^{i\frac{2\pi l}{N}}-1]} \sum_{n=0}^{N-1} \varepsilon'_{n+1} e^{i\sum_{j=0}^{n}\varepsilon'_j} \big[1 - e^{i\frac{2\pi l(n+1)}{N}}\big], \tag{53}$$

where, for $l<0$, we define $s_l = s_{N-l}$. Clearly, $\{s_l\}_{0<|l|\le N/2}$ now is an i.i.d. sequence of random variables with the same distribution as s_1. Here we note that we have, for N even, counted a term too many. However, for this term, we have that $l = \frac{N}{2}$, so that the difference is equal to, with $l = \frac{N}{2}$,

$$\begin{aligned} &\frac{is_l}{N[e^{i\frac{2\pi l}{N}}-1]} \sum_{n=0}^{N-1} \varepsilon'_{n+1} e^{i\sum_{j=0}^{n}\varepsilon'_j} \big[1 - e^{i\frac{2\pi l(n+1)}{N}}\big] \\ &\quad = \frac{is_l}{2N} \sum_{n=0}^{N-1} \varepsilon'_{n+1} e^{i\sum_{j=0}^{n}\varepsilon'_j} \big[(-1)^n - 1\big] \xrightarrow{P} 0, \end{aligned} \tag{54}$$

so that this change is negligible. From now on, we will for convenience define

$$\xi' = \sum_{0<|l|\le N/2} \frac{is_l}{N[e^{i\frac{2\pi l}{N}}-1]} \sum_{n=0}^{N-1} \varepsilon'_{n+1} e^{i\sum_{j=0}^{n}\varepsilon'_j} \big[1 - e^{i\frac{2\pi l(n+1)}{N}}\big]. \tag{55}$$

When $N \to \infty$, we see that for every l fixed,

$$N[e^{i\frac{2\pi l}{N}} - 1] \to 2\pi l i, \tag{56}$$

so that it is natural to assume that

$$\xi' \approx \sum_{l\in\mathbb{Z}:l\neq 0} \frac{s_l}{2\pi l} \sum_{n=0}^{N-1} \varepsilon'_{n+1} e^{i\sum_{j=0}^{n}\varepsilon'_j} \big[1 - e^{i\frac{2\pi l(n+1)}{N}}\big]. \tag{57}$$

To make this precise, we define

$$S(t) = \sum_{l\in\mathbb{Z}:l\neq 0} \frac{s_l}{2\pi l} \big[1 - e^{i2\pi lt}\big]. \tag{58}$$

This random sum is a well-defined random variable, and, in particular, has finite second moment. We will show below that

$$\zeta = \sigma \int_0^1 e^{i\sigma B_t} S(t) dB_t, \tag{59}$$

and we will also prove that $\xi' \xrightarrow{P} \zeta$, by using (59). First, with

$$S_N(t) = \sum_{0<|l|\le N/2} \frac{is_l}{N[e^{i\frac{2\pi l}{N}}-1]} \big[1 - e^{i2\pi lt}\big], \tag{60}$$

we have

$$\xi' = \sum_{n=0}^{N-1} \varepsilon'_{n+1} e^{i\sum_{j=0}^{n}\varepsilon'_j} S_N\left(\frac{n+1}{N}\right). \tag{61}$$

We will prove that $\xi \xrightarrow{P} \zeta$ in two steps, namely, with δ_N and γ_N given by

$$\delta_N = \sum_{n=0}^{N-1} \varepsilon'_{n+1} e^{i\sum_{j=0}^{n}\varepsilon'_j} \left[S_N\left(\frac{n+1}{N}\right) - S\left(\frac{n+1}{N}\right)\right] \tag{62}$$

and

$$\gamma_N = \sum_{n=0}^{N-1} \varepsilon'_{n+1} e^{i\sum_{j=0}^{n}\varepsilon'_j} S\left(\frac{n+1}{N}\right) - \zeta, \tag{63}$$

we have that

$$\xi = \zeta + \eta_N + \delta_N + \gamma_N. \tag{64}$$

Therefore, it suffices to prove (52) and (59) and

$$\delta_N \xrightarrow{P} 0, \tag{65}$$

as well as

$$\gamma_N \xrightarrow{P} 0. \tag{66}$$

Together, these claims prove Theorem 3.1. Equations (52), (59), (65) and (66) will be proved below. The above completes the proof of Theorem 3.1 subject to (52), (59), (65) and (66). ■

Subsequently, we prove the technical results (52), (59), (65) and (66). We make frequent use of the fact that, for a sequence of (complex) random variables Y_N, the convergence $Y_N \xrightarrow{P} 0$ follows if $\mathbb{E}[|Y_N|^2] \to 0$. This is follows from the Chebychev inequality, as well as

$$\lim_{N\to\infty} \mathbb{P}(|Y_N| > \epsilon) \le \lim_{N\to\infty} \mathbb{E}[|Y_N|^2] = 0. \tag{67}$$

For convenience, we will prove the statements in the order (65), (52), (59) and (66).

Proof of (65). We bound the second moment of the summands with $|l| > K$, for any K, by

$$\begin{aligned} &\mathbb{E}\left[\Big| \sum_{K\le|l|\le N/2} \frac{is_l}{N[e^{i\frac{2\pi l}{N}}-1]} \right. \\ &\qquad \left. \cdot \sum_{n=0}^{N-1} \varepsilon'_{n+1} e^{i\sum_{j=0}^{n}\varepsilon'_j} \big[1 - e^{i\frac{2\pi l(n+1)}{N}}\big] \Big|^2 \right] \\ &\le \sigma_s^2 \sum_{K\le|l|\le N/2} \frac{1}{N^2|e^{i\frac{2\pi l}{N}}-1|^2} \mathbb{E}\left[\Big| \sum_{n=0}^{N-1} \varepsilon'_{n+1} e^{i\sum_{j=0}^{n}\varepsilon'_j}\Big|^2\right], \end{aligned} \tag{68}$$

where we use the independence of s_l for different l, and we write $\sigma_s^2 = \mathbb{E}[|s_l|^2]$. We write out

$$\begin{aligned} &\mathbb{E}\left[\Big| \sum_{n=0}^{N-1} \varepsilon'_{n+1} e^{i\sum_{j=0}^{n}\varepsilon'_j}\Big|^2\right] \\ &\quad = \sum_{n_1=0}^{N-1}\sum_{n_2=0}^{N-1} \mathbb{E}\big[\varepsilon'_{n_1+1}\varepsilon'_{n_2+1} e^{i\sum_{j=0}^{n_1}\varepsilon'_j} e^{-i\sum_{j=0}^{n_2}\varepsilon'_j}\big]. \end{aligned} \tag{69}$$

When $n_1 < n_2$, we have that ε'_{n_2+1} is independent of $\varepsilon'_{n_1+1}e^{i\sum_{j=0}^{n_1}\varepsilon'_j}e^{-i\sum_{j=0}^{n_2}\varepsilon'_j}$, so that the expected value equals zero. Therefore, we arrive at

$$\mathbb{E}\left[\Big|\sum_{n=0}^{N-1}\varepsilon'_{n+1}e^{i\sum_{j=0}^{n}\varepsilon'_j}\Big|^2\right]=\sum_{n=0}^{N-1}\mathbb{E}\big[\varepsilon'^2_{n+1}\big]=\sigma^2, \quad (70)$$

so that we obtain

$$\mathbb{E}\left[\Big|\sum_{K\le|l|\le N/2}\frac{is_l}{N[e^{i\frac{2\pi l}{N}}-1]}\cdot\sum_{n=0}^{N-1}\varepsilon'_{n+1}e^{i\sum_{j=0}^{n}\varepsilon'_j}\big[1-e^{i\frac{2\pi l(n+1)}{N}}\big]\Big|^2\right]\le\sigma_s^2\sigma^2\sum_{K\le|l|\le N/2}\frac{1}{N^2|e^{i\frac{2\pi l}{N}}-1|^2}. \quad (71)$$

It is not hard to see that when $|l|\ge\frac{N}{4}$, we have that

$$|e^{i\frac{2\pi l}{N}}-1|\ge\left|1-\cos\left(\frac{2\pi l}{N}\right)\right|\ge 1. \quad (72)$$

Furthermore, using the fact that $|\sin(x)|\ge\frac{2|x|}{\pi}$ for all $|x|\le\frac{\pi}{2}$, we obtain that for $|l|\le\frac{N}{4}$

$$|e^{i\frac{2\pi l}{N}}-1|\ge\left|\sin\left(\frac{2\pi l}{N}\right)\right|\ge\frac{4|l|}{N}. \quad (73)$$

We conclude that

$$|e^{i\frac{2\pi l}{N}}-1|\ge\min\left\{\frac{|l|}{N},1\right\}. \quad (74)$$

As a consequence, we obtain that

$$\mathbb{E}\left[\Big|\sum_{K\le|l|\le N/2}\frac{is_l}{N[e^{i\frac{2\pi l}{N}}-1]}\cdot\sum_{n=0}^{N-1}\varepsilon'_{n+1}e^{i\sum_{j=0}^{n}\varepsilon'_j}\big[1-e^{i\frac{2\pi l(n+1)}{N}}\big]\Big|^2\right]\le\sigma_s^2\sigma^2\sum_{K\le|l|\le N/2}\frac{1}{\min\{|l|^2,N^2\}}, \quad (75)$$

so that, uniformly in N, the variance of the summands with $|l|>K$ is bounded by a constant times K^{-1}. Therefore, when $K=K_N$ tends to infinity, the variance of this term tends to zero, so that this term tends to zero in probability by (67). An identical computation shows that

$$\mathbb{E}\left[\Big|\sum_{K_N\le|l|<\infty}\frac{s_l}{2\pi l}\sum_{n=0}^{N-1}\varepsilon'_{n+1}e^{i\sum_{j=0}^{n}\varepsilon'_j}\big[1-e^{i\frac{2\pi l(n+1)}{N}}\big]\Big|^2\right]\to 0, \quad (76)$$

which implies that the contribution due to $|l|\ge K_N$ in ζ converge to 0 in probability. We are left to investigate the contribution due to $0<|l|\le K_N$, since we know that

$$\delta_N-\delta'_N\xrightarrow{P}0, \quad (77)$$

where we define

$$\delta'_N=\sum_{1<|l|\le K_N}s_l\left[\frac{i}{N[e^{i\frac{2\pi l}{N}}-1]}-\frac{1}{2\pi l}\right]\cdot\sum_{n=0}^{N-1}\varepsilon'_{n+1}e^{i\sum_{j=0}^{n}\varepsilon'_j}\big[1-e^{i\frac{2\pi l(n+1)}{N}}\big]. \quad (78)$$

Therefore, it suffices to prove that

$$\delta'_N\xrightarrow{P}0. \quad (79)$$

For this, we note that

$$\delta'_N=\sum_{1<|l|\le K_N}s_l\frac{\big[2\pi il-N[e^{i\frac{2\pi l}{N}}-1]\big]}{N[e^{i\frac{2\pi l}{N}}-1](2\pi l)}\cdot\sum_{n=0}^{N-1}\varepsilon'_{n+1}e^{i\sum_{j=0}^{n}\varepsilon'_j}\big[1-e^{i\frac{2\pi l(n+1)}{N}}\big]. \quad (80)$$

We can compute similarly to (71) that

$$\mathbb{E}[|\delta'_N|^2]=\sigma_s^2\sigma^2\sum_{1<|l|\le K_N}\frac{\big|2\pi il-N[e^{i\frac{2\pi l}{N}}-1]\big|^2}{N^2|e^{i\frac{2\pi l}{N}}-1|^2(2\pi l)^2}. \quad (81)$$

A Taylor expansion yields that

$$|2\pi il-N[e^{i\frac{2\pi l}{N}}-1]|\le C\frac{l^2}{N}, \quad (82)$$

Therefore, also using (73), we arrive at

$$\mathbb{E}[|\delta'_N|^2]\le C\sigma_s^2\sigma^2\sum_{1<|l|\le K_N}\frac{1}{N}\le\frac{cK_N}{N}. \quad (83)$$

This converges to zero for every $K_N=o(N)$, for example for $K_N=\sqrt{N}$. This proves the convergence in (65). ■

Proof of (52). Recall that

$$\eta_N=\frac{1}{N}\sum_{0<|l|\le N/2}\frac{s_l}{e^{i\frac{2\pi l}{N}}-1}\cdot\sum_{n=0}^{N-1}\big[e^{i\varepsilon'_{n+1}}-1-i\varepsilon'_{n+1}\big]e^{i\sum_{j=0}^{n}\varepsilon'_j}\big[1-e^{i\frac{2\pi l(n+1)}{N}}\big]. \quad (84)$$

We show that $\mathbb{E}[|\eta_N|]^2$ converges to zero, which implies that η_N converges to zero in probability by (67). To prove that the second moment of η_N converges to zero, we use the computations in the proof of (65) to obtain that

$$\mathbb{E}[|\eta_N|^2]\le\sigma_s^2\sum_{0<|l|\le N/2}\frac{1}{N^2|e^{i\frac{2\pi l}{N}}-1|^2}\cdot\mathbb{E}\left[\Big|\sum_{n=0}^{N-1}\big[e^{i\varepsilon'_{n+1}}-1-i\varepsilon'_{n+1}\big]e^{i\sum_{j=0}^{n}\varepsilon'_j}\Big|^2\right]. \quad (85)$$

Similarly to (70), we obtain that

$$\mathbb{E}\left[\Big|\sum_{n=0}^{N-1}\left[e^{i\varepsilon'_{n+1}}-1-i\varepsilon'_{n+1}\right]e^{i\sum_{j=0}^{n}\varepsilon'_j}\Big|^2\right] = \sum_{n=0}^{N-1}\mathbb{E}\left[\left|e^{i\varepsilon'_{n+1}}-1-i\varepsilon'_{n+1}\right|^2\right] \le \sum_{n=0}^{N-1}\mathbb{E}\left[\varepsilon'^4_{n+1}\right]=\frac{3\sigma^4}{N}, \quad (86)$$

where we use that $\mathbb{E}\left[\varepsilon'^4_{n+1}\right]=\frac{3\sigma^4}{N^2}$. We arrive at

$$\mathbb{E}[\eta_N^2] \le \frac{3\sigma^4\sigma_s^2}{N}\sum_{0<|l|\le N/2}\frac{1}{N^2|e^{i\frac{2\pi l}{N}}-1|^2} \le \frac{c}{N}, \quad (87)$$

using a similar argument as in (75) with $K=1$, where c is a constant. This proves that the approximation in (52) is valid, and even shows that the error in the approximation is, with high probability, smaller than $N^{-\frac{1}{2}+\delta}$ and any $\delta>0$. ■

Proof of (59). This again follows from a second moment calculation. We can interchange the order of summation when we have a finite sum, but for an *infinite* sum that is not so clear. However, by a similar computation as in the proof of (65), we see that

$$\sigma\int_0^1 e^{i\sigma B_t}(S(t)-S_{\le K_N}(t))dB_t \xrightarrow{P} 0, \quad (88)$$

where

$$S_{\le K_N}(t)=\sum_{0<|l|\le K_N}\frac{s_l}{2\pi l}\left[1-e^{i2\pi lt}\right]. \quad (89)$$

Also, it is not hard to see that, again using a second moment computation,

$$\sum_{|l|>K_N}\frac{\sigma s_l}{2\pi l}\int_0^1 e^{i\sigma B_t}[1-e^{i2\pi lt}]dB_t \xrightarrow{P} 0. \quad (90)$$

Noting that

$$\zeta=\sigma\int_0^1 e^{i\sigma B_t}S(t)dB_t+\sum_{|l|>K_N}\frac{\sigma s_l}{2\pi l}\int_0^1 e^{i\sigma B_t}[1-e^{i2\pi lt}]dB_t - \sigma\int_0^1 e^{i\sigma B_t}(S(t)-S_{\le K_N}(t))dB_t \quad (91)$$

then completes the proof. ■

Proof of (66). We use that $\varepsilon'_j=\sigma\left[B_{\frac{j+1}{N}}-B_{\frac{j}{N}}\right]$, where $\{B_t\}_{t\ge 0}$ is a standard Brownian motion. Then,

$$\sum_{n=0}^{N-1}\varepsilon'_{n+1}e^{i\sum_{j=0}^{n}\varepsilon'_j}S\left(\frac{n+1}{N}\right) = \sigma\sum_{n=0}^{N-1}e^{i\sigma B_{\frac{n+1}{N}}}S\left(\frac{n+1}{N}\right)\left[B_{\frac{n+2}{N}}-B_{\frac{n+1}{N}}\right] = \sigma\sum_{n=1}^{N}e^{i\sigma B_{\frac{n}{N}}}S\left(\frac{n}{N}\right)\left[B_{\frac{n+1}{N}}-B_{\frac{n}{N}}\right]. \quad (92)$$

The above is the usual approximation to the stochastic integral

$$\sigma\int_0^1 e^{i\sigma B_t}S(t)dB_t. \quad (93)$$

Since, for every t, the integrand $e^{i\sigma B_t}S(t)$ has a finite second moment, and since the process $t\mapsto e^{i\sigma B_t}S(t)$ is predictable, the sum in (92) converges in probability to the integral in (93). See, e.g., [24, Section 13.8] for convergence results of stochastic integrals. ■

ACKNOWLEDGEMENTS

The authors are grateful to the anonymous referees for their valuable comments.

REFERENCES

[1] S. Weinstein and P. Ebert, "Data transmission by frequency-division multiplexing using the discrete fourier transform," *IEEE Trans. Commun.*, vol. 19, pp. 628–634, Oct. 1971.

[2] A. Peled and A. Ruiz, "Frequency domain data transmission using reduced computational complexity algorithms," in *IEEE International Conf. Acoust., Speech, Signal Processing*, Apr. 1980, vol. 5, pp. 964–967.

[3] IEEE 802.11a standard, ISO/IEC 802-11:1999/Amd 1:2000(E).

[4] IEEE Standard for Local and Metropolitan Area Networks Part 16: Air Interface for Fixed Broadband Wireless Access Systems, IEEE Std 802.16-2004, 2004.

[5] European Telecommunications Standard Institute ETSI, Radio Broadcasting Systems; Digital Audio Broadcasting (DAB) to mobile, portable and fixed receiver, EN 300 401 V1.3.1, Apr. 2000.

[6] European Telecommunications Standard Institute ETSI, Digital Video Broadcasting (DVB); Framing structure, channel coding and modulation for digital terrestrial television, EN 300 744 V1.2.1, July 1999.

[7] T. Pollet, M. van Bladel, and M. Moeneclaey, "BER sensitivity of OFDM systems to carrier frequency offset and Wiener phase noise," *IEEE Trans. Commun.*, vol. 43, no. 2/3/4, pp. 191–193, Feb./Mar./Apr. 1995.

[8] P. Robertson and S. Kaiser, "Analysis of the effects of phase-noise in orthogonal frequency division multiplex (OFDM) systems," in *Proc. IEEE ICC*, June 1995, vol. 3, pp. 1652–1657.

[9] L. Tomba, "Analysis of phase noise effects in OFDM modems," *IEEE Trans. Commun.*, vol. 46, no. 5, pp. 580–583, May 1998.

[10] A. G. Armada, "Understanding the effects of phase noise in orthogonal frequency division multiplexing (OFDM)," *IEEE Trans. Broadcasting*, vol. 47, no. 2, pp. 153–159, June 2001.

[11] S. Wu and Y. Bar-Ness, "Performance analysis on the effect of phase noise in OFDM systems," in *Proc. IEEE 7th International Symposium Spread Spectrum Techniques Apps.*, Sep. 2002, vol. 1, pp. 133–138.

[12] H. Nikookar and R. Prasad, "On the sensitivity of multicarrier transmission over multipath channels to phase noise and frequency offset," in *Proc. 7th IEEE International Symposium Personal, Indoor Mobile Radio Commun.*, Oct. 1996, vol. 1, pp. 68–72.

[13] H. Steendam, M. Moeneclaey, and H. Sari, "The effect of carrier phase jitter on the performance of orthogonal frequency-division multiple-access systems," *IEEE Trans. Commun.*, vol. 46, no. 4, pp. 456–459, Apr. 1998.

[14] L. Piazzo and P. Mandarini, "Analysis of phase noise effects in OFDM modems," *IEEE Trans. Commun.*, vol. 50, no. 10, pp. 1696–1705, Oct. 2002.

[15] D. Petrovic, W. Rave, and G. Fettweis, "Properties of the intercarrier interference due to phase noise in OFDM," in *Proc. IEEE ICC*, May 2005, vol. 4, pp. 2605–2610.

[16] V. S. Abhayawardhana and I. J. Wassell, "Common phase error correction with feedback for OFDM in wireless communication," in *Proc. IEEE Globecom*, Nov. 2002, vol. 1, pp. 651–655.

[17] D. Petrovic, W. Rave, and G. Fettweis, "Common phase error due to phase noise in OFDM - estimation and suppression," in *Proc. IEEE PIMRC*, Sep. 2004, pp. 1901–1905.

[18] R. A. Casas, S. L. Biracree, and A. E. Youtz, "Time domain phase noise correction for OFDM signals," *IEEE Trans. Broadcasting*, vol. 48, no. 3, pp. 230–236, Sep. 2002.

[19] D. Petrovic, W. Rave, and G. Fettweis, "Intercarrier interference due to Phase Noise in OFDM - estimation and suppression," in *Proc. IEEE VTC Fall*, Sep. 2004, pp. 1901–1905.

[20] M. Lax, "Classical noise. V. Noise in self-sustained oscillators," *Phys. Rev.*, vol. 160, pp. 290–307, Aug. 1967.
[21] A. Demir, A. Mehrotra, and J. Roychowdhury, "Phase noise in oscillators: A unifying theory and numerical methods for characterization," *IEEE Trans. Circuits Syst. I*, pp. 655–674, May 2000.
[22] J. G. Proakis, *Digital Communications*, 3rd ed. New York: McGraw-Hill, 1995.
[23] M. K. Simon and M. S. Alouni, *Digital Communication over Fading Channels, A Unified Approach to Performance Analysis*. New York: Wiley, 2000.
[24] G. Grimmett and D. Stirzaker, *Probability and Random Processes*, 3rd. ed. Oxford, UK: Oxford University Press, 2001.
[25] B. Øksendahl, *Stochastic Differential Equations*, 5th ed. Berlin: Springer, 2000.

Tim C. W. Schenk (S'01-M'07) was born in Heerle, The Netherlands, on June 28, 1978. He received the M.Sc. and Ph.D. degree in electrical engineering from Eindhoven University of Technology (TU/e), Eindhoven, The Netherlands, in 2002 and 2006, respectively. The research for this Ph.D. thesis was focussed on the influence and digital compensation of RF impairments in multiple antenna and multi-carrier systems. From 2002 to 2004 he was with the Wireless Systems Research group of Agere Systems in Nieuwegein, The Netherlands. From 2004 to 2006 he was a research assistant in the Radiocommunication group of TU/e. During the first part of 2006 he was a visiting researcher at CEA-LETI in Grenoble, France. In October 2006 he joined the Connectivity Systems and Networks department of Philips Research Laboratories, Eindhoven, The Netherlands as a research scientist.

Dr. Schenk is a member of the Royal Institute of Engineers (KIVI-NIRIA) in The Netherlands and the Dutch Electronics and Radio Society (NERG).

Remco W. van der Hofstad was born in Eindhoven, The Netherlands, on May 3, 1971. He received his M.Sc. degree with honors at the Department of Mathematics of the University of Utrecht in 1993, where he subsequently continued with his Ph.D. He received his Ph.D. degree in 1997 on research in statistical physics concerning random polymers. In the following year, he was a post-doc at McMaster University in Hamilton, Canada, and worked at Microsoft Research in Redmond, U.S.A. In 1998, he obtained an assistant professor position at Delft University of Technology, and in 2002 an associate professorship at Eindhoven University of Technology, where, in January 2005, he was promoted to full professor in probability. Since January 2004, he also acts as one of the scientific advisors in the Random Spatial Structures program in the European research institute in probability and statistics EURANDOM, which is located on the campus of Eindhoven University of Technology. His research is in applications of probability, mostly in statistical physics and in telecommunications. His research interests include large deviation theory, self-interacting stochastic processes and random walks, random graphs and complex networks, percolation and interacting particle systems.

Erik R. Fledderus received the M.Sc. (cum laude) and Ph.D. degrees in Applied Mathematics from Twente University of Technology, Enschede, The Netherlands, in 1993 and 1997, respectively. From 1997 onwards, he was with KPN Research (now TNO Information and Communication Technology), Leidschendam, The Netherlands, and from 2003 he is part-time professor with the Radiocommunications group of Eindhoven University of Technology in the area of wireless communications networks. His research interests and publications are in the areas of design and simulation of radio networks, smart antennas and propagation modelling. At TNO Information and Communication Technology, Prof. Fledderus is manager of the "Next Generation ICT infrastructures" program.

Peter F. M. Smulders (S'82-M'82-SM'98) graduated from Eindhoven University of Technology in 1985. In 1985 he joined the Propagation and Electromagnetic Compatibility Department of the Research Neher Laboratories of the Netherlands PTT. During that time he was doing research in the field of compromising emanation from civil data processing equipment. In 1988 he moved to the Eindhoven University of Technology as a staff member of the Telecommunication Division. Next to his lecturing duties he performed a Ph.D. research in the field of 60 GHz broadband wireless LANs. His current work addresses the feasibility of low-cost, low power small sized wireless LAN technology operating in the 60 GHz frequency band. With this low-cost technology it should be possible to serve an unprecedented maximum user data rate in the order of Gbps.

He is senior member of IEEE and his research interest that covers 60 GHz physical and higher layers is reflected in numerous IEEE publications. He was involved in various research projects addressing 60 GHz antennas and interworking (ACTS, MEDIAN) and 60 GHz propagation (MinEZ, Broadband Radio@Hand). Currently, he is also addressing baseband design in the context of 60 GHz radio (Freeband, Wicomm). As project manager of the SiGi Spot project his future research activities will range from 60 GHz physical layer design to associated network aspects.